

A Novel Method to Measure Glucose Uptake and Myosin Heavy Chain Isoform Expression of Single Fibers From Rat Skeletal Muscle

James G. MacKrell^{1,2} and Gregory D. Cartee^{1,2,3}

Skeletal muscle includes many individual fibers with diverse phenotypes. A barrier to understanding muscle glucose uptake at the cellular level has been the absence of a method to measure glucose uptake by single fibers from mammalian skeletal muscle. This study's primary objective was to develop a procedure to measure glucose uptake by single fibers from rat skeletal muscle. Rat epitrochlearis muscles were incubated *ex vivo* with [³H]-2-deoxy-D-glucose, with or without insulin or AICAR, before isolation of ~10–30 single fibers from each muscle. Fiber type (myosin heavy chain [MHC] isoform) and glucose uptake were determined for each single fiber. Insulin-stimulated glucose uptake (which was cytochalasin B inhibitable) varied according to MHC isoform expression, with ~2-fold greater values for IIA versus IIB or IIX fibers and ~1.3-fold greater for hybrid (IIB/X) versus IIB fibers. In contrast, AICAR-stimulated glucose uptake was ~1.5-fold greater for IIB versus IIA fibers. A secondary objective was to assess insulin resistance of single fibers from obese versus lean Zucker rats. Genotype differences were observed for insulin-stimulated glucose uptake and inhibitor κ B (I κ B)- β abundance in single fibers (obese less than lean), with decrements for glucose uptake (44–58%) and I κ B- β (25–32%) in each fiber type. This novel method creates a unique opportunity for future research focused on understanding muscle glucose uptake at the cellular level. *Diabetes* 61:995–1003, 2012

Skeletal muscle is the major tissue for insulin-mediated disposal of blood glucose (1). Accordingly, the capacity for insulin-stimulated glucose disposal by skeletal muscle is a crucial determinant of glucose regulation. However, glucose uptake is not uniform across all muscles (2). Even when muscles are studied *ex vivo* to minimize the direct effects of microvascular perfusion and muscle contractile activity, muscle-dependent differences in glucose uptake remain (3).

Each muscle includes hundreds or thousands of cells known as muscle fibers. There can be substantial heterogeneity in the metabolic characteristics of individual fibers within a particular muscle (4). The gold standard for classifying fiber type relies on identifying the myosin heavy chain (MHC) isoform(s) expressed by each fiber (5). The MHC isoforms expressed by adult rat muscle fibers are types I, IIA, IIB, and IIX (6–9). Many rat skeletal muscles contain moderate to high proportions of two or more of the

MHC isoforms (10–13). However, in a few rat muscles or regions of muscles, a single MHC isoform accounts for 80–90% of the total MHC expression. Henriksen et al. (3) studied isolated rat muscles with diverse fiber-type compositions. They reported similar insulin-stimulated glucose uptake for soleus (predominantly type I) compared with flexor digitorum longus (FDB; predominantly type IIA) (3). The insulin-stimulated glucose uptake for the soleus or FDB was approximately twofold greater than the predominantly type IIB epitrochlearis (3).

The study of cultured myocytes has provided important insights into mechanisms that regulate glucose uptake (14–20). However, because cultured cells fail to replicate all properties of adult muscle, the ability to measure glucose uptake by single fibers from authentic muscle would prove valuable. No methods are available for measuring glucose uptake by single fibers from mammalian muscle. To fully understand muscle glucose uptake at the cellular level, it will be essential to develop such a method. Therefore, our first aim was to develop and validate a novel method to measure glucose uptake by single fibers from rat muscle. Because the results from muscle tissue research provide evidence that glucose uptake capacity varies according to fiber type, it was important to also identify the MHC isoform expressed in the same fibers used for glucose uptake measurements. We hypothesized that insulin-stimulated glucose uptake would vary among the fibers, with fibers expressing type I or IIA MHC having greater values than fibers expressing IIB or IIX MHC. Our second aim was to use the single-fiber glucose uptake method to gain insights into insulin resistance by measuring glucose uptake of single fibers from obese Zucker (OZ) versus lean Zucker (LZ) rats. We hypothesized that when single fibers expressing the same MHC isoform were compared, insulin-stimulated glucose uptake for fibers from LZ rats would exceed the values for fibers from OZ rats.

RESEARCH DESIGN AND METHODS

Materials. Human recombinant insulin was from Eli Lilly (Indianapolis, IN). AICAR and cytochalasin B (CB) were from Calbiochem/EMD Chemicals (Gibbstown, NJ). Reagents for SDS-PAGE and immunoblotting were from Bio-Rad (Hercules, CA). Bicinchoninic acid protein assay reagent and tissue protein extraction reagent (T-PER) were from Pierce Biotechnology (Rockford, IL). [³H]-2-Deoxy-D-glucose ([³H]-2-DG) was from PerkinElmer Life and Analytical Sciences (Waltham, MA). Collagenase (type II) was from Worthington Biochem (Lakewood, NJ). Trypan Blue was from Invitrogen (Carlsbad, CA). Other reagents were from Sigma-Aldrich (St. Louis, MO) or Fisher Scientific (Pittsburgh, PA). Reagents and apparatus for SDS-PAGE and immunoblotting were purchased from Bio-Rad. West Dura Extended Duration Substrate was from Pierce Biotechnology. Anti-APPL1 (adaptor protein containing pH domain, PTB domain, and leucine zipper motif) antibody (no. ab59592) was from Abcam (Cambridge, MA), anti-inhibitor κ B (I κ B)- β antibody (no. sc-945) was from Santa Cruz (Santa Cruz, CA), and anti-rabbit IgG horseradish peroxidase (no. 7074) was from Cell Signaling Technology (Danvers, MA).

From the ¹Muscle Biology Laboratory, School of Kinesiology, University of Michigan, Ann Arbor, Michigan; the ²Department of Molecular and Integrative Physiology, University of Michigan, Ann Arbor, Michigan; and the ³Institute of Gerontology, University of Michigan, Ann Arbor, Michigan.

Corresponding author: Gregory D. Cartee, gcartee@umich.edu.

Received 14 September 2011 and accepted 8 January 2012.

DOI: 10.2337/db11-1299

© 2012 by the American Diabetes Association. Readers may use this article as long as the work is properly cited, the use is educational and not for profit, and the work is not altered. See <http://creativecommons.org/licenses/by-nc-nd/3.0/> for details.

Animal treatment. Procedures for animal care were approved by the University of Michigan Committee on Use and Care of Animals. Male Wistar rats (aged 7–10 weeks) were from Harlan (Indianapolis, IN). Lean (Fa^{+/+}) and obese (fa/fa) male Zucker rats (aged 7–8 weeks) were from Charles River Laboratories (Wilmington, MA). Animals were provided with rodent chow ad libitum until 1700 h the night before the experiment when food was removed. The next day, between 1000 and 1300 h, rats were anesthetized (intraperitoneal injection of sodium pentobarbital), and both epitrochlearis muscles were extracted.

Muscle incubation. Isolated muscles underwent a series of incubation steps (see below). Unless otherwise noted, vials were shaken (45 rpm), gassed (95% O₂/5% CO₂), and heated (35°C) in a water bath.

Standard incubation protocol. Isolated muscles were incubated in vials containing 2 mL media 1 (Krebs Henseleit buffer [KHB] supplemented with 0.1% bovine serum albumin [BSA] [KHB-BSA], 2 mmol/L sodium pyruvate, and 6 mmol/L mannitol) with 0 or 12 nmol/L insulin for 20 min. Each muscle was then transferred to a second vial for a 60-min incubation in 2 mL media 2 (KHB-BSA, 1 mmol/L 2-DG [specific activity of 0.225 mCi/mmol [³H]-2-DG], and 9 mmol/L mannitol [specific activity of 0.022 mCi/mmol [¹⁴C]mannitol]) and the same insulin concentration as the previous step. Muscles were blotted, freeze clamped, and stored at –80°C.

Revised incubation protocol. Isolated muscles were incubated in vials containing 2 mL media 1 with 0 or 12 nmol/L insulin for 20 min. Each muscle was transferred to a second vial for a 60-min incubation in 2 mL media 3 (KHB-BSA, 1 mmol/L 2-DG [specific activity of 13.5 mCi/mmol [³H]-2-DG], and 9 mmol/L mannitol) and the same insulin concentration as the previous step. Muscles underwent 3 × 5-min washes (100 rpm) in ice-cold KHB-BSA to clear extracellular space of 2-DG (22). Muscles were placed in collagenase media (Ca²⁺-free KHB and 1.5% type II collagenase) for 60 min for enzymatic digestion of collagen (enzymatically digested muscles are hereafter referred to as fiber bundles). Some muscles were incubated with CB (25 μmol/L in 0.4% DMSO). One muscle per rat was incubated with CB for sequential incubations in media 1 and media 3. The contralateral muscle served as a control (vehicle, 0.4% DMSO). CB or vehicle remained at the same concentration in incubation media 1 and media 3. Some muscles were incubated with 2 mmol/L AICAR using the revised protocol described above, except that AICAR was substituted for insulin.

Single-fiber isolation and processing. Following collagenase incubation, fiber bundles were removed from solution, washed with Ca²⁺-free KHB, and placed in a Petri dish containing Ca²⁺-free KHB plus Trypan Blue (0.25%). Under a dissecting microscope, single fibers were teased from the bundle using forceps. Only fibers nonpermeable to Trypan Blue (Trypan Blue-permeable fibers were very rare) were isolated (~10–30 fibers per fiber bundle). Each fiber was imaged using a camera-enabled microscope with Leica Application Suite EZ software after isolation. Fiber dimensions were measured using Image J software. The width (mean value for width measured at three locations per fiber: near the fiber midpoint and approximately halfway between the midpoint and each end of the fiber) and length of each fiber were used to estimate volume ($V = \pi r^2 l$, where r refers to radius as determined by half of the width measurement and l refers to length). Following imaging, each fiber was transferred by pipette with 10 μL solution to a microcentrifuge tube containing 40 μL of lysis buffer (T-PER, 1 mmol/L EDTA, 1 mmol/L EGTA, 2.5 mmol/L sodium pyrophosphate, 1 mmol/L Na₂VO₄, 1 mmol/L β-glycerophosphate, 1 μg/mL leupeptin, and 1 mmol/L phenylmethylsulfonyl fluoride). Laemmli buffer (2 ×, 50 μL) was added to each tube. Tubes were vortexed. Aliquots of lysed fiber were used for 2-DG uptake and MHC characterization.

Single-fiber 2-DG uptake. An aliquot of the lysed fiber was pipetted into a vial with 10 mL scintillation cocktail. Aliquots of media 3 (in which muscles had been incubated with [³H]-2-DG) and Ca²⁺-free KHB (used to isolate fibers) were added to separate vials containing 10 mL scintillation cocktail. [³H]-2-DG disintegrations per minute (dpm) for each vial were determined using a scintillation counter. ³H dpm accumulation was calculated as fiber ³H dpm minus ³H dpm in Ca²⁺-free KHB rinse solution. This difference was used as the corrected dpm value to calculate 2-DG accumulation by fibers essentially as previously performed for muscles (23,24)

$$\text{corrected total } ^3\text{H dpm per fiber} \times \frac{\mu\text{mol 2-DG per mL incubation media}}{^3\text{H dpm per mL incubation media}}$$

Measured 2-DG accumulation was normalized to calculated fiber volume and expressed as nanomoles per microliter.

MHC isoform expression. MHC isoforms were separated and identified by SDS-PAGE (25). An aliquot of fiber homogenate was run on gels at constant voltage (70 V) for ~24 h. A mixture of homogenized soleus and extensor digitorum longus muscles (containing all four MHC isoforms) was used as a standard on each gel. Gels were stained with Coomassie Brilliant Blue for ~1 h and destained in 20% methanol and 10% acetic acid mixture.

Immunoblotting. Before immunoblotting, epitrochlearis single-fiber lysates from LZ and OZ rats were fiber typed based on MHC expression. Relative protein

abundance of each fiber was calculated using a three-point MHC standard curve from soleus and extensor digitorum longus muscles lysate loaded on each gel. A similar amount of MHC protein for each fiber sample was loaded onto 9% SDS-PAGE. Following electrophoretic transfer to nitrocellulose, gels were stained with Coomassie Brilliant Blue, and posttransfer MHC bands were quantified by densitometry (AlphaEase FC; AlphaInnotech, San Leandro, CA), as previously described (26). After immunoblotting the membranes, the immunoreactive protein bands (IκB-β and APPL1) were visualized by enhanced chemiluminescence and quantified by densitometry, as previously described (27). IκB-β and APPL1 protein levels for each fiber were expressed relative to the fiber's respective posttransfer MHC density.

Muscle and fiber-bundle homogenization. Intact muscles and fiber bundles used for 2-DG uptake were processed in 1 mL ice-cold lysis buffer using glass-on-glass grinding tubes. Homogenates were rotated (4°C, 1 h) before being centrifuged (12,000g, 10 min, 4°C). Aliquots of supernatant used for 2-DG uptake were pipetted into vials for scintillation counting, and 2-DG uptake was determined. A portion of supernatant was used to determine protein concentration (bicinchoninic acid protein assay). 2-DG uptake was normalized to either muscle weight (micromoles per gram for intact muscles) or protein content (micromoles per microgram of protein for fiber bundles). Remaining supernatant was stored at –80°C until further analysis.

Statistical analysis. Data are expressed as means ± SEM. Differences between the two groups were determined by the Student *t* test. The Pearson correlation coefficient was used for correlation analysis. One-way ANOVA was used to evaluate the effect of fiber type on 2-DG uptake. Two-way ANOVA was used for the CB experiment and the Zucker rat experiment. The Tukey post hoc *t* test was applied to determine the source of significant variance. A *P* value of ≤0.05 was considered statistically significant.

RESULTS

2-DG values were similar for whole muscles using revised versus standard protocols. The standard incubation protocol for 2-DG uptake uses [¹⁴C]mannitol to calculate extracellular space, which is used to calculate extracellular 2-DG, which is subtracted from whole-muscle 2-DG to calculate intracellular 2-DG accumulation (24). To confirm that the standard versus revised protocols resulted in similar values for 2-DG uptake, paired muscles from Wistar rats were studied with both protocols. Both muscles from some rats were incubated with insulin, and both muscles from other rats were incubated without insulin. KHB was supplemented with [³H]-2-DG and [¹⁴C]mannitol for one muscle, whereas KHB was supplemented with [³H]-2-DG only for the contralateral muscle. The muscle incubated in [¹⁴C]mannitol and [³H]-2-DG was immediately freeze clamped following incubation, whereas the contralateral muscle (incubated in [³H]-2-DG only) underwent three rinses (5 min each) in ice-cold KHB. 2-DG uptake did not differ significantly between muscles incubated using the standard versus revised protocol (Fig. 1A). 2-DG values were significantly correlated (basal: $R = 0.88$, $P < 0.05$; insulin stimulated: $R = 0.91$, $P < 0.05$) between paired muscles undergoing the standard versus revised protocol (Fig. 1B). 2-DG uptake for muscles undergoing the standard protocol also can be expressed as nanomoles per microliter: basal 1.86 ± 0.41 nmol/μL and insulin stimulated 5.89 ± 0.82 nmol/μL.

Incubation with collagenase did not alter 2-DG uptake. Paired muscles were dissected from Wistar rats. Both muscles from some rats were incubated with insulin, and both muscles from other rats were incubated without insulin. KHB was supplemented with [³H]-2-DG for the second incubation step. After three rinses to remove extracellular 2-DG, one muscle per rat was incubated with collagenase, and the other was incubated without collagenase. Collagenase did not alter 2-DG uptake (Fig. 1C). **Insulin-stimulated 2-DG uptake by single fibers was correlated with 2-DG for fiber bundles.** 2-DG that enters muscle fibers is rapidly phosphorylated by hexokinase, whereas resultant 2-DG-6P is trapped intracellularly

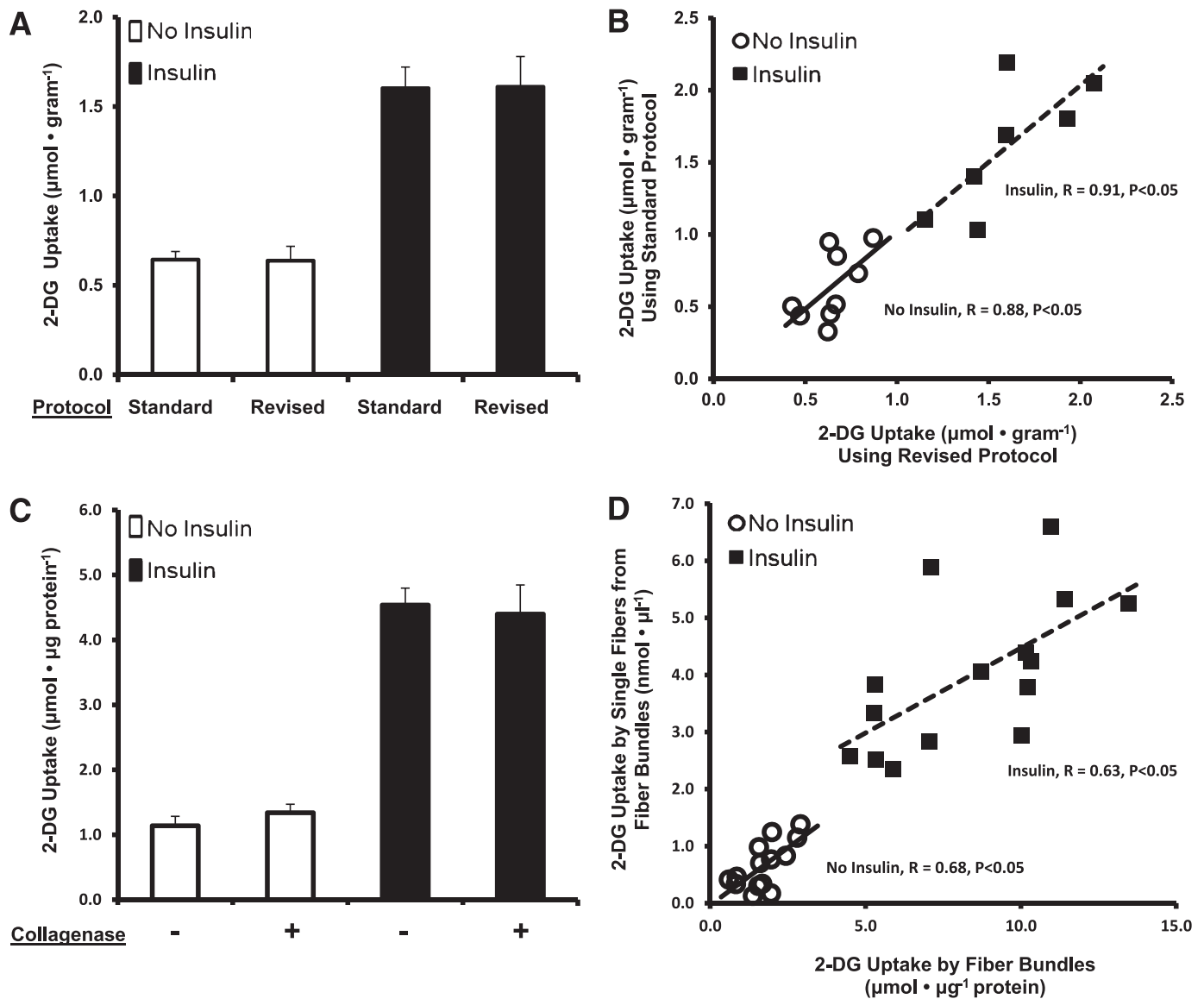


FIG. 1. A: 2-DG uptake by epitrochlearis muscle with (■) or without (□) insulin stimulation. Paired epitrochlearis muscles from the same rat underwent either the standard incubation protocol ($[^3\text{H}]\text{-2-DG}$ and $[^{14}\text{C}]\text{mannitol}$) or the revised incubation protocol ($[^3\text{H}]\text{-2-DG}$ only, with three washes). Data are means \pm SEM ($n = 7\text{--}9$ muscles per protocol at each insulin concentration). B: Correlations between the standard and revised protocols from muscles used in A ($n = 7\text{--}9$ muscles per protocol and insulin concentration). Each symbol represents data from paired muscles after incubation in the respective protocol, with (■) or without (○) insulin. Without insulin: $R = 0.88$, $P < 0.05$; with insulin: $R = 0.91$, $P < 0.05$. C: 2-DG uptake by epitrochlearis muscles with (■) or without (□) insulin stimulation, followed by a 60-min incubation in media with (+) or without (-) collagenase. Data are means \pm SEM ($n = 6$ per bar). D: Correlations between the 2-DG uptake by fiber bundles (expressed as micromoles per microgram protein) vs. mean 2-DG uptake by single fibers isolated from their corresponding fiber bundle ($\sim 10\text{--}20$ fibers, expressed as nanomoles per microliter), represented by each symbol, with (■) or without (○) insulin. Without insulin: $R = 0.68$, $P < 0.05$; with insulin: $R = 0.63$, $P < 0.05$.

without further metabolism. After collagenase treatment, muscles from Wistar rats were incubated in Ca^{2+} -free KHB with Trypan Blue. A bundle of several hundred fibers from each muscle used to harvest single fibers also was processed for 2-DG uptake without insulin or with 12 nmol/L insulin. 2-DG uptake also was determined from $\sim 10\text{--}30$ single fibers per bundle. Figure 1D illustrates the significant correlations (basal: $R = 0.68$, $P < 0.05$; insulin stimulated: $R = 0.63$, $P < 0.05$) between mean 2-DG uptake by single fibers from each bundle versus 2-DG uptake by the donor bundle from which fibers were isolated.

Differences in insulin-stimulated 2-DG uptake by single fibers. Relative numbers of fibers (%) for each MHC isoform in single fibers isolated from Wistar rats were 9% IIA, 61% IIB, 8% IIX, and 22% IIB/X (see Fig. 2 for representative gel).

These values compare with the relative abundance of MHC composition of whole epitrochlearis muscles from 7- to 10-week-old Wistar rats (8% I, 13% IIA, 51% IIB, and 28% IIX) (10). Figure 3A illustrates data from single fibers from Wistar rats used to measure both insulin-stimulated 2-DG uptake and MHC isoform expression. We found no significant fiber-type differences for basal 2-DG uptake. ANOVA revealed a significant difference ($P < 0.05$) for insulin-stimulated 2-DG uptake of IIA fibers versus fibers expressing each of the other MHC isoforms, and a significant difference between IIB/X versus IIB fibers (IIB/X greater than IIB).

Insulin-stimulated 2-DG uptake by single fibers was inhibited by CB. For 2-DG uptake by single fibers from muscles incubated without insulin, there were significant main effects ($P < 0.05$) of CB and fiber type. The only

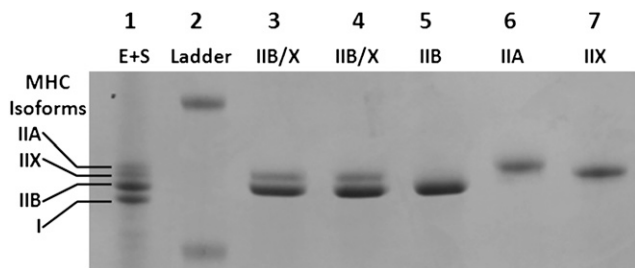


FIG. 2. Representative SDS-polyacrylamide gel of single fibers isolated from rat epitrochlearis muscle visualized using Coomassie Brilliant Blue staining. *Lane 1:* E+S, pooled sample from rat extensor digitorum longus and soleus muscles expressing MHC types I, IIA, IIB, and IIX. *Lane 2:* Ladder, molecular mass standard. *Lane 3:* Epitrochlearis single fiber expressing type IIB/X (hybrid fiber). *Lane 4:* Epitrochlearis single fiber expressing type IIB/X (hybrid fiber). *Lane 5:* Epitrochlearis single fiber expressing type IIB. *Lane 6:* Epitrochlearis single fiber expressing type IIA. *Lane 7:* Epitrochlearis single fiber expressing type IIX.

statistically significant difference ($P < 0.05$) identified by post hoc analysis was in IIB/X fibers (no CB greater than with CB) (Fig. 3B). For 2-DG uptake by single fibers from insulin-stimulated muscles, there was a significant main effect of CB ($P < 0.001$). Post hoc analysis ($P < 0.001$) indicated that values without CB exceeded values with CB for each fiber type. For 2-DG uptake by single fibers from insulin-stimulated muscles, there was a significant main effect of fiber type ($P < 0.001$) and a significant interaction between CB status and fiber type ($P < 0.001$). Post hoc analysis indicated that for insulin-stimulated muscles incubated without CB, 2-DG values for IIA fibers were significantly ($P < 0.05$) greater than values for all other fiber types, and 2-DG values for IIB/X fibers were significantly ($P < 0.05$) greater than values for IIB fibers. For 2-DG uptake by single fibers from muscles incubated with insulin and CB, post hoc analysis detected no significant differences among fiber types.

AICAR-stimulated 2-DG uptake by single fibers. Figure 4 illustrates data from single fibers used to measure AICAR-stimulated 2-DG uptake and MHC isoform expression. There were no significant fiber-type differences for basal 2-DG uptake. ANOVA revealed a significant difference ($P < 0.05$) for AICAR-stimulated 2-DG uptake between fiber types. Post hoc analysis indicated a significant difference for IIB fibers versus IIA fibers (IIB greater than IIA).

2-DG uptake by single fibers from epitrochlearis of OZ versus LZ rats. Basal 2-DG uptake values by single fibers were not significantly different between OZ and LZ rats, regardless of MHC isoform expression (Fig. 5). For 2-DG uptake by single fibers from insulin-stimulated muscles, there was a significant main effect of genotype ($P < 0.001$), and post hoc analysis indicated that insulin-stimulated 2-DG values for each fiber type were significantly greater for LZ versus OZ rats ($P < 0.05$). For 2-DG uptake by single fibers from insulin-stimulated muscles, there also was a significant main effect of fiber type ($P < 0.001$) and a significant interaction (genotype \times fiber type; $P < 0.001$). Post hoc analysis indicated that within the LZ fibers from insulin-stimulated muscles, 2-DG uptake for IIA fibers exceeded values for all other fiber types ($P < 0.05$). However, for single fibers from insulin-stimulated OZ muscles, post hoc analysis did not reveal significant differences among fiber types. Relative decrements for 2-DG uptake of insulin-stimulated OZ versus LZ muscles were estimated by calculating differences between the mean LZ

value for each fiber type and individual OZ values for the same fiber type. Calculated reductions for insulin-stimulated 2-DG uptake for the fiber types (IIB: $44.4 \pm 3.0\%$, IIA: $58.0 \pm 10.0\%$, IIX: $52.0 \pm 8.01\%$, and IIB/X: $52.3 \pm 5.0\%$) did not differ significantly.

I κ B- β and APPL1 abundance in single fibers. For I κ B- β , we observed a significant main effect of genotype ($P < 0.005$; LZ greater than OZ), regardless of fiber type. No fiber-type difference for I κ B- β was detected, and the calculated reductions in I κ B- β content for LZ versus OZ were similar across fiber types (IIB: $24.8 \pm 10.7\%$, IIA: $27.5 \pm 7.1\%$, IIX: $30.0 \pm 9.1\%$, and IIB/X: $31.9 \pm 4.0\%$) (Fig. 6A). For APPL1, there was no significant genotype or fiber-type difference (Fig. 6B).

DISCUSSION

Skeletal muscle is a heterogeneous tissue primarily composed of muscle fibers that can have diverse phenotypes. However, there was previously no method to evaluate glucose uptake by single mammalian fibers. The current study filled this gap. It is noteworthy that the novel method includes identification of MHC isoform expression in each fiber used for the glucose uptake assay. The results indicated that insulin-stimulated glucose uptake varied among fibers according to fiber type, with twofold greater insulin-mediated glucose uptake for IIA versus IIB or IIX fibers. These data extend earlier research using tissue analyses in which rat muscles primarily composed of IIA fibers had approximately two- to threefold greater insulin-mediated glucose uptake than muscles mostly composed of IIB fibers (3). The current results also revealed that hybrid fibers, which expressed more than one MHC isoform (IIB/X), had higher insulin-induced glucose uptake than IIB fibers. These results are important because hybrid fibers can be abundant in rat muscle (28,29) and novel because conventional tissue analysis cannot assess the glucose uptake by hybrid fibers. In contrast to the results of insulin-stimulated glucose uptake, AICAR-stimulated glucose uptake was greater in IIB versus IIA fibers. These data coincide with results for whole epitrochlearis (predominantly IIB) that had greater AICAR-stimulated glucose uptake versus whole FDB (predominantly IIA) (30). The relative magnitude of insulin resistance in OZ versus LZ rats was substantial (from 44 to 58% for fibers expressing each of the fiber types evaluated: IIA, IIB, IIX, and IIB/X). Furthermore, for OZ versus LZ rats I κ B- β content also was reduced (25–32%) across each fiber type.

We performed a series of experiments to validate the procedure for assessing glucose uptake by single fibers. We demonstrated that glucose uptake was unaltered by collagenase treatment and documented that glucose uptake by single fibers was highly correlated with values for donor muscles from which single fibers were isolated. Using CB, a compound that inhibits glucose transporter protein-mediated glucose transport, we established that 2-DG accumulation by single fibers was attributable to transporter-specific glucose uptake.

The MHC isoform profile of single fibers isolated from Wistar rats (9% IIA, 61% IIB, 8% IIX, and 22% IIB/X) compares to the relative abundance of the MHC composition of whole epitrochlearis from Wistar rats (8% I, 13% IIA, 51% IIB, and 28% IIX) (10). It is uncertain why type I fibers were not included among the hundreds of fibers isolated using collagenase. It may relate to the greater collagen levels surrounding type I compared with type II fibers in rat muscle

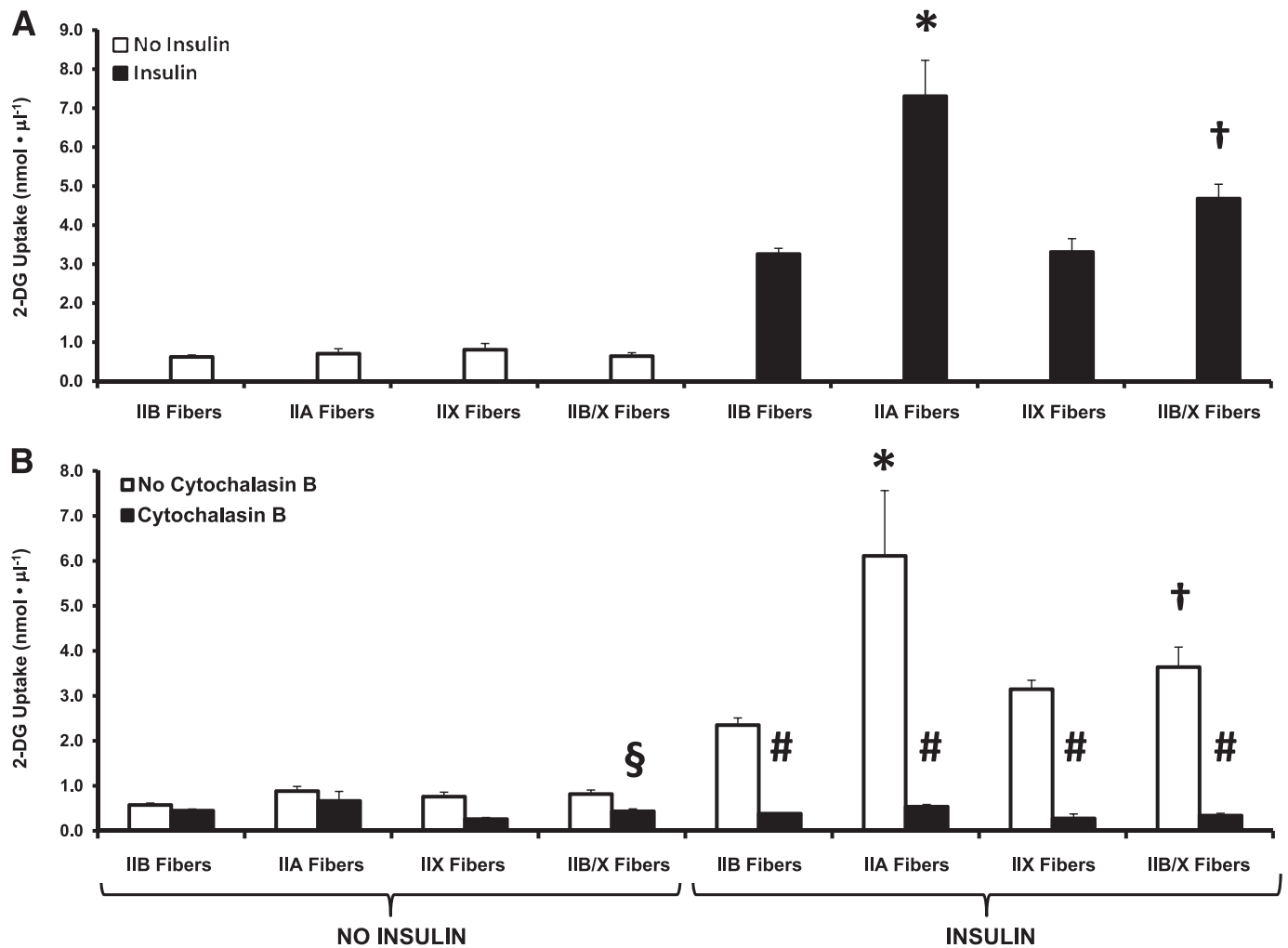


FIG. 3. A: Mean 2-DG uptake by fibers expressing the same MHC isoform, with (■) or without (□) insulin stimulation. For basal (no insulin) fibers, the number of fibers for each MHC type is in parentheses: IIB (105), IIA (16), IIX (7), and IIB/X (30). For insulin-stimulated fibers, the number of fibers for each MHC type is in parentheses: IIB (117), IIA (15), IIX (13), and IIB/X (41). Data are means \pm SEM. ANOVA revealed a significant difference related to MHC expression for insulin-stimulated fibers ($P < 0.05$). Post hoc analysis of insulin-stimulated fibers revealed significant differences ($P < 0.05$) for 1) *IIA vs. all other fiber types; and 2) †IIB/X vs. IIB fibers. **B:** Mean 2-DG uptake by fibers isolated from epitrochlearis muscle that were incubated without (□) or with (■) CB. For basal (no insulin) fibers, without CB, the number of fibers for each MHC type is in parentheses: IIB (58), IIA (6), IIX (11), and IIB/X (25). For insulin-stimulated fibers, without CB, the number of fibers for each MHC type is in parentheses: IIB (37), IIA (5), IIX (6), and IIB/X (19). For insulin-stimulated fibers, with CB, the number of fibers for each MHC type is in parentheses: IIB (40), IIA (6), IIX (5), and IIB/X (16). Data are means \pm SEM. For fibers without insulin, there were significant main effects of CB status (no CB greater than with CB; $P < 0.001$) and fiber type ($P < 0.001$). Post hoc analysis indicated for fibers without insulin, no CB is greater than with CB for IIB/X fibers (§ $P < 0.05$). For fibers with insulin, there were significant main effects of CB status (no CB greater than with CB; $P < 0.001$) and fiber type ($P < 0.001$) and a significant CB \times fiber-type interaction ($P < 0.001$). Post hoc analysis revealed that for insulin-stimulated fibers 1) # $P < 0.05$ for CB vs. no CB for all fiber types; and 2) for fibers with no CB, * $P < 0.05$ for IIA vs. IIB, IIX, and IIB/X fibers and † $P < 0.05$ for IIB/X vs. IIB fibers.

(31). Consistent with this interpretation, despite repeated attempts to use collagenase with isolated soleus, a muscle composed of ~90% type I fibers (10), we were unable to isolate any single fibers. Regardless, the protocol successfully isolated single fibers expressing each of the other MHC isoforms (representing >90% of MHC expressed by the epitrochlearis) in proportions roughly comparable to their respective abundance in whole epitrochlearis.

Glucose uptake measurement by traditional tissue analysis has limitations that are avoided using the single-fiber method. 1) No muscles in rats have been found to exclusively express a single MHC isoform. Therefore, tissue comparisons are limited to muscles or regions of muscles largely composed of a particular fiber type. 2) No rat muscle has been identified in which type IIX fibers account for most of the MHC. 3) Tissue analysis cannot reveal the glucose

uptake of hybrid fibers. 4) Tissue analysis includes the contribution of other cell types in skeletal muscle (vascular, neural, adipose, fibroblasts, etc.). 5) Various conditions alter fiber-type composition of muscles (32–36), confounding interpretation of between-group comparisons. The single-fiber procedure makes comparisons possible between fibers matched for MHC expression.

Full understanding of muscle insulin resistance will require elucidation of insulin resistance at the cellular level. Cultured myocytes provide valuable insights into the mechanisms for insulin resistance (37–39); however, they are imperfect models of fibers in adult muscle. To probe muscle insulin resistance, we compared glucose uptake in single fibers from LZ and OZ rats. Insulin-stimulated glucose uptake is reduced by 67% in isolated intact epitrochlearis (40). Using the perfused rat hind-limb procedure, Sherman

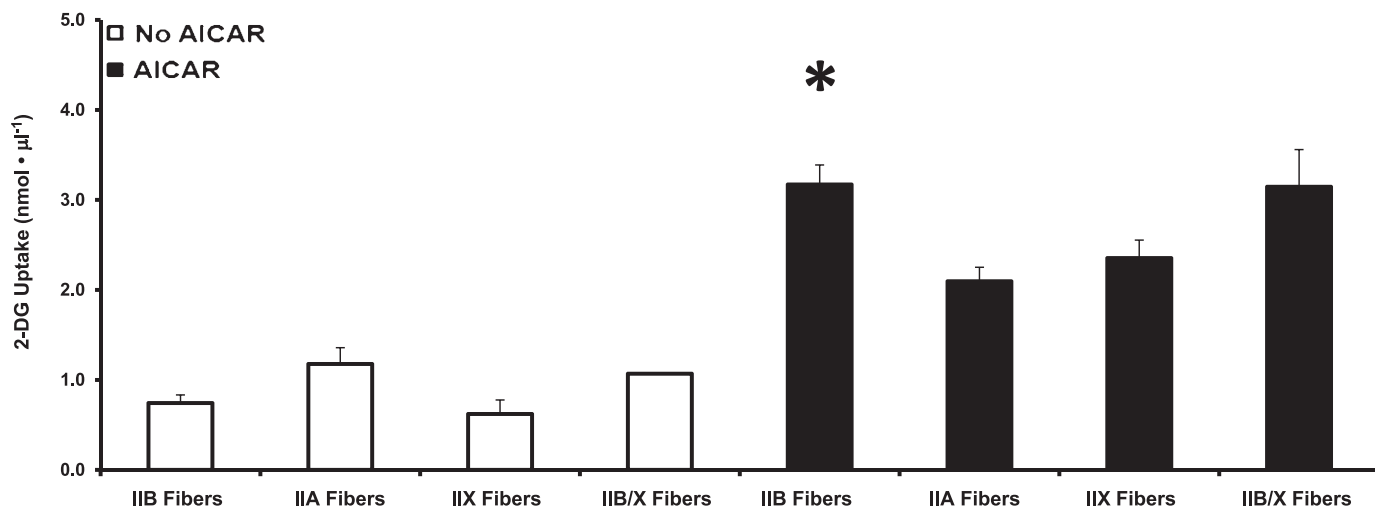


FIG. 4. Mean 2-DG uptake by fibers expressing the same MHC isoform, with (■) or without (□) AICAR stimulation. For basal (no AICAR) fibers, the number of fibers for each MHC type is within parentheses: IIB (27), IIA (6), IIX (6), and IIB/X (1). For AICAR-stimulated fibers, the number of fibers for each MHC type is within parentheses: IIB (51), IIA (21), IIX (13), and IIB/X (15). Data are means ± SEM. ANOVA revealed a significant difference related to MHC expression for AICAR-stimulated fibers ($P < 0.05$). Post hoc analysis of AICAR-stimulated fibers revealed a significant difference. * $P < 0.05$ for IIB vs. IIA fibers.

et al. (41) found similar relative deficits for OZ versus LZ rats in glucose uptake for a muscle composed of predominantly type I fibers (soleus, 47% decline), a region of muscle with a high portion of IIA fibers (red quadriceps, 66% decline), and a region of muscle that is mostly IIB fibers (white quadriceps, 54% decline). In single fibers that expressed known MHC isoforms, the relative decrements were similar to these published results for tissue glucose uptake. Furthermore, the relative decrements were similar for each fiber type that was assessed. The results from perfused and isolated muscles indicate that all fiber types contribute to the insulin resistance in OZ rats.

The correspondence for the magnitude of insulin resistance in single fibers compared with published data for isolated epitrochlearis and perfused hind limb (40,41) provides further support for the validity of the single-fiber method. However, various interventions, including exercise, dietary manipulations, or pharmaceutical treatments, may not uniformly modulate single-fiber glucose uptake. The single-fiber method could be especially valuable for experiments using vivo gene delivery (by electroporation or gene gun) to muscle. These approaches have provided important information about the regulation of muscle glucose uptake. However, because gene delivery using

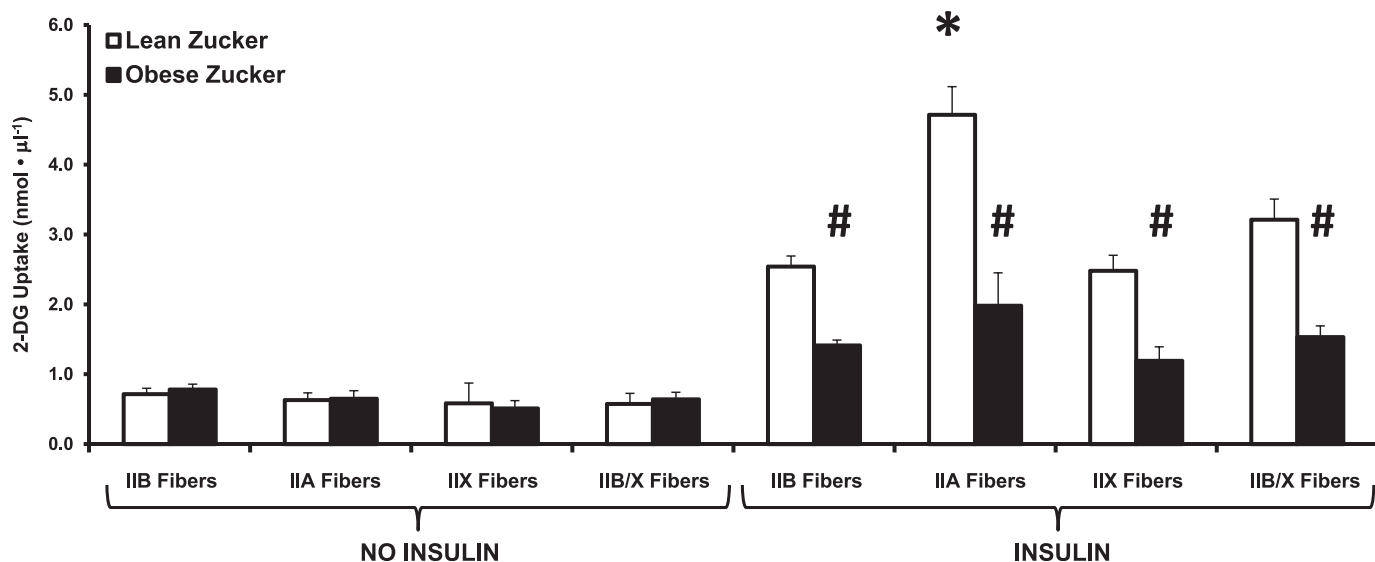


FIG. 5. Mean 2-DG uptake by fibers isolated from epitrochlearis muscles from lean Zucker (LZ) (□) or obese Zucker (OZ) (■) rats. For basal (no insulin) fibers from LZ rat muscles, the number of fibers for each MHC type is in parentheses: IIB (51), IIA (10), IIX (8), and IIB/X (11). For basal fibers from OZ rat muscles, the number of fibers for each MHC type is in parentheses: IIB (71), IIA (10), IIX (5), and IIB/X (14). For insulin-stimulated fibers, from LZ rat muscles, the number of fibers for each MHC type is in parentheses: IIB (73), IIA (13), IIX (15), and IIB/X (19). For insulin-stimulated fibers from OZ rat muscles, the number of fibers for each MHC type is in parentheses: IIB (99), IIA (9), IIX (7), and IIB/X (25). Data are means ± SEM. For fibers with insulin, there were significant main effects of genotype (LZ greater than OZ; $P < 0.001$) and fiber type ($P < 0.001$) and a significant genotype × fiber-type interaction ($P < 0.01$). Post hoc analysis of insulin-stimulated fibers revealed 1) # $P < 0.05$ for insulin-stimulated OZ vs. LZ for all fiber types; and 2) for insulin-stimulated fibers within only the LZ group, * $P < 0.05$ for insulin-stimulated IIA vs. IIB, IIX, and IIB/X fibers.

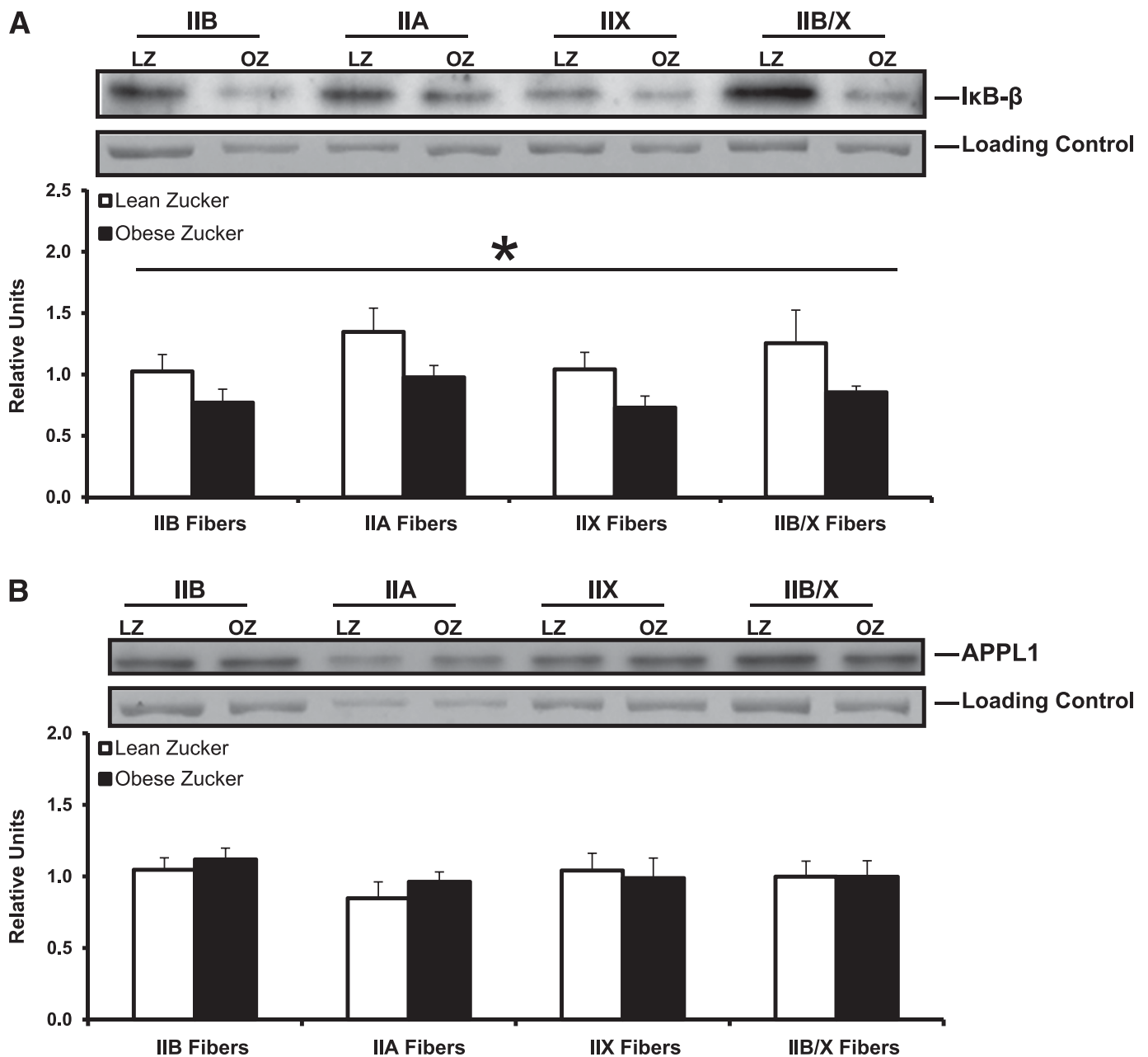


FIG. 6. IκB-β (*A*) and APPL1 (*B*) protein abundance in single fibers isolated from epitrochlearis muscles from LZ (□) or OZ (■) rats. Representative blots of protein abundance (IκB-β or APPL1) and corresponding Coomassie Brilliant Blue-stained gels of posttransfer MHC (loading control) are provided. The density value for each protein (IκB-β or APPL1) was normalized to the density value for the loading control. *A*: There was a significant main effect of genotype (LZ greater than OZ; * $P < 0.005$) but no significant fiber-type difference for IκB-β. Data are means \pm SEM. $n = 8$ fibers per bar. *B*: There was no significant genotype or fiber-type difference for APPL1. Data are means \pm SEM. $n = 8$ fibers per bar.

these approaches is not 100% efficient, the interpretation can be imprecise. For example, if gene delivery induces a 50% reduction in glucose uptake, it is possible that only 50% of the fibers were transfected, and glucose uptake was completely inhibited in each transfected fiber. Alternatively, it is possible that most of the fibers were transfected, but glucose uptake was only partly inhibited in each transfected fiber. The single-fiber method can turn this complication into an advantage by allowing isolation of those fibers expressing the gene of interest (facilitated by a fluorescent reporter). Moreover, the nontransfected fibers could provide an invaluable internal control from the same muscle. It also is possible that transfection efficiency will vary by fiber type or that the consequences of

transfection will be fiber-type specific. The single-fiber model offers the opportunity to address these possible outcomes.

Obesity-associated inflammation is considered a likely contributor to muscle insulin resistance (42,43). Overactivation of the IκB/nuclear factor-κB (NFκB) pathway is hypothesized to trigger insulin resistance, and reduced IκB-β protein abundance commonly is used as a marker of this activation. For example, IκB-β content was decreased in muscle of insulin-resistant humans with type 2 diabetes (44). Previous studies using whole skeletal muscles or regions of muscles have suggested that activation of the IκB/NFκB pathway may be modulated by obesity in a fiber-type-dependent manner (45,46). The current results demonstrate

significantly lower I κ B- β levels in single fibers from obese rats, regardless of fiber type. When these novel observations are coupled with our demonstrated decline in glucose uptake by single fibers from OZ rats, the results provide new evidence that supports the idea that the insulin resistance found in fibers from the obese rats, regardless of fiber type, is linked to greater activation of the I κ B/NF κ B pathway. Another novel result was the lack of a significant fiber-type difference for I κ B- β levels, indicating that the fiber-type differences in glucose transport are independent of differences in the expression of this protein. APPL1 mediates adiponectin signaling and has been linked to enhanced insulin-stimulated Akt activation, GLUT4 translocation, and glucose uptake (47,48). The lack of significant effects of either obesity or fiber type on APPL1 abundance, taken together with the single-fiber glucose uptake data, demonstrate that neither the obesity-related insulin resistance nor the fiber-type differences in glucose uptake are attributable to differential expression of this regulatory protein.

In conclusion, the current study provides new insights into the relationship between MHC isoform expression and glucose uptake in rat muscle. In addition, the results demonstrated that in OZ rats, the extent of insulin resistance was similar for single fibers expressing different MHC isoforms. More importantly, the study validated an innovative approach that has the potential to provide unique information about muscle glucose uptake to be used for understanding, preventing and treating insulin resistance.

ACKNOWLEDGMENTS

This research was supported by grants from the National Institutes of Health (DK-071771 and AG-10026 to G.D.C.).

No potential conflicts of interest relevant to this article were reported.

J.G.M. researched data, contributed to the discussion, and wrote, reviewed, and edited the manuscript. G.D.C. contributed to the discussion and wrote, reviewed, and edited the manuscript. G.D.C. is the guarantor of this work and, as such, had full access to all of the data in the study and takes responsibility for the integrity of the data and the accuracy of the data analysis.

The authors thank Edward Arias (University of Michigan) for his assistance with the muscle dissections.

REFERENCES

- DeFronzo RA. Lilly Lecture 1987: The triumvirate: beta-cell, muscle, liver: a collusion responsible for NIDDM. *Diabetes* 1988;37:667–687
- James DE, Jenkins AB, Kraegen EW. Heterogeneity of insulin action in individual muscles in vivo: euglycemic clamp studies in rats. *Am J Physiol* 1985;248:E567–E574
- Henriksen EJ, Bourey RE, Rodnick KJ, Koranyi L, Permutt MA, Holloszy JO. Glucose transporter protein content and glucose transport capacity in rat skeletal muscles. *Am J Physiol* 1990;259:E593–E598
- Pette D, Staron RS. Mammalian skeletal muscle fiber type transitions. *Int Rev Cytol* 1997;170:143–223
- Pandorf CE, Caiozzo VJ, Haddad F, Baldwin KM. A rationale for SDS-PAGE of MHC isoforms as a gold standard for determining contractile phenotype. *J Appl Physiol* 2010;108:222–222; author reply 226
- Bigard AX, Sanchez H, Birot O, Serrurier B. Myosin heavy chain composition of skeletal muscles in young rats growing under hypobaric hypoxia conditions. *J Appl Physiol* 2000;88:479–486
- Schiaffino S, Reggiani C. Molecular diversity of myofibrillar proteins: gene regulation and functional significance. *Physiol Rev* 1996;76:371–423
- Schiaffino S, Reggiani C. Myosin isoforms in mammalian skeletal muscle. *J Appl Physiol* 1994;77:493–501
- Thomason DB, Baldwin KM, Herrick RE. Myosin isozyme distribution in rodent hindlimb skeletal muscle. *J Appl Physiol* 1986;60:1923–1931
- Castorena CM, Mackrell JG, Bogan JS, Kanzaki M, Cartee GD. Clustering of GLUT4, TUG and RUVBL2 protein levels correlate with myosin heavy chain isoform pattern in skeletal muscles, but AS160 and TBC1D1 levels do not. *J Appl Physiol*. 28 July 2011 [Epub ahead of print]
- Sullivan VK, Powers SK, Criswell DS, Tumer N, Larochelle JS, Lowenthal D. Myosin heavy chain composition in young and old rat skeletal muscle: effects of endurance exercise. *J Appl Physiol* 1995;78:2115–2120
- Adams GR, Baldwin KM. Age dependence of myosin heavy chain transitions induced by creatine depletion in rat skeletal muscle. *J Appl Physiol* 1995;78:368–371
- Ogura Y, Naito H, Kakigi R, et al. Different adaptations of alpha-actinin isoforms to exercise training in rat skeletal muscles. *Acta Physiol (Oxf)* 2009;196:341–349
- Huang C, Thirone AC, Huang X, Klip A. Differential contribution of insulin receptor substrates 1 versus 2 to insulin signaling and glucose uptake in I6 myotubes. *J Biol Chem* 2005;280:19426–19435
- Sarabia V, Lam L, Burdett E, Leiter LA, Klip A. Glucose transport in human skeletal muscle cells in culture. Stimulation by insulin and metformin. *J Clin Invest* 1992;90:1386–1395
- Klip A, Ramlal T, Bilan PJ, Marette A, Liu Z, Mitsumoto Y. What signals are involved in the stimulation of glucose transport by insulin in muscle cells? *Cell Signal* 1993;5:519–529
- Sargeant R, Mitsumoto Y, Sarabia V, Shillabeer G, Klip A. Hormonal regulation of glucose transporters in muscle cells in culture. *J Endocrinol Invest* 1993;16:147–162
- Klip A, Tsakiridis T, Marette A, Ortiz PA. Regulation of expression of glucose transporters by glucose: a review of studies in vivo and in cell cultures. *FASEB J* 1994;8:43–53
- Foster LJ, Klip A. Mechanism and regulation of GLUT-4 vesicle fusion in muscle and fat cells. *Am J Physiol Cell Physiol* 2000;279:C877–C890
- Krook A, Zierath JR. Specificity of insulin signalling in human skeletal muscle as revealed by small interfering RNA. *Diabetologia* 2009;52:1231–1239
- Edman KA. Contractile performance of striated muscle. *Adv Exp Med Biol* 2010;682:7–40
- Wang C. Insulin-stimulated glucose uptake in rat diaphragm during post-natal development: lack of correlation with the number of insulin receptors and of intracellular glucose transporters. *Proc Natl Acad Sci U S A* 1985;82:3621–3625
- Cartee GD, Bohn EE. Growth hormone reduces glucose transport but not GLUT-1 or GLUT-4 in adult and old rats. *Am J Physiol* 1995;268:E902–E909
- Hansen PA, Gulve EA, Holloszy JO. Suitability of 2-deoxyglucose for in vitro measurement of glucose transport activity in skeletal muscle. *J Appl Physiol* 1994;76:979–985
- Talmadge RJ, Roy RR. Electrophoretic separation of rat skeletal muscle myosin heavy-chain isoforms. *J Appl Physiol* 1993;75:2337–2340
- Murphy RM. Enhanced technique to measure proteins in single segments of human skeletal muscle fibers: fiber-type dependence of AMPK-alpha1 and -beta1. *J Appl Physiol* 2011;110:820–825
- Sharma N, Arias EB, Bhat AD, et al. Mechanisms for increased insulin-stimulated Akt phosphorylation and glucose uptake in fast- and slow-twitch skeletal muscles of calorie-restricted rats. *Am J Physiol Endocrinol Metab* 2011;300:E966–E978
- DeNardi C, Ausoni S, Moretti P, et al. Type 2X-myosin heavy chain is coded by a muscle fiber type-specific and developmentally regulated gene. *J Cell Biol* 1993;123:823–835
- Stephenson GM. Hybrid skeletal muscle fibres: a rare or common phenomenon? *Clin Exp Pharmacol Physiol* 2001;28:692–702
- Ai H, Ihlemann J, Hellsten Y, et al. Effect of fiber type and nutritional state on AICAR- and contraction-stimulated glucose transport in rat muscle. *Am J Physiol Endocrinol Metab* 2002;282:E1291–E1300
- Kovanen V, Suominen H, Heikkinen E. Collagen of slow twitch and fast twitch muscle fibres in different types of rat skeletal muscle. *Eur J Appl Physiol Occup Physiol* 1984;52:235–242
- Pellegrino MA, D'Antona G, Bortolotto S, et al. Clenbuterol antagonizes glucocorticoid-induced atrophy and fibre type transformation in mice. *Exp Physiol* 2004;89:89–100
- Schiaffino S, Sandri M, Murgia M. Activity-dependent signaling pathways controlling muscle diversity and plasticity. *Physiology (Bethesda)* 2007;22:269–278
- Baldwin KM, Haddad F. Effects of different activity and inactivity paradigms on myosin heavy chain gene expression in striated muscle. *J Appl Physiol* 2001;90:345–357
- Diffey GM, McCue S, LaRosa A, Herrick RE, Baldwin KM. Interaction of various mechanical activity models in regulation of myosin heavy chain isoform expression. *J Appl Physiol* 1993;74:2517–2522

36. Diffie GM, Caiozzo VJ, McCue SA, Herrick RE, Baldwin KM. Activity-induced regulation of myosin isoform distribution: comparison of two contractile activity programs. *J Appl Physiol* 1993;74:2509–2516
37. Zierath JR, He L, Gumà A, Odegaard Wahlström E, Klip A, Wallberg-Henriksson H. Insulin action on glucose transport and plasma membrane GLUT4 content in skeletal muscle from patients with NIDDM. *Diabetologia* 1996;39:1180–1189
38. Klip A, Ramlal T, Walker D. Insulin stimulation of glucose uptake and the transmembrane potential of muscle cells in culture. *FEBS Lett* 1986;205:11–14
39. Sarabia V, Ramlal T, Klip A. Glucose uptake in human and animal muscle cells in culture. *Biochem Cell Biol* 1990;68:536–542
40. Etgen GJ Jr, Wilson CM, Jensen J, Cushman SW, Ivy JL. Glucose transport and cell surface GLUT-4 protein in skeletal muscle of the obese Zucker rat. *Am J Physiol* 1996;271:E294–E301
41. Sherman WM, Katz AL, Cutler CL, Withers RT, Ivy JL. Glucose transport: locus of muscle insulin resistance in obese Zucker rats. *Am J Physiol* 1988;255:E374–E382
42. Gregor MF, Hotamisligil GS. Inflammatory mechanisms in obesity. *Annu Rev Immunol* 2011;29:415–445
43. Schenk S, Saberi M, Olefsky JM. Insulin sensitivity: modulation by nutrients and inflammation. *J Clin Invest* 2008;118:2992–3002
44. Sriwijitkamol A, Christ-Roberts C, Berria R, et al. Reduced skeletal muscle inhibitor of κB β content is associated with insulin resistance in subjects with type 2 diabetes: reversal by exercise training. *Diabetes* 2006;55:760–767
45. Bhatt BA, Dube JJ, Dedousis N, Reider JA, O'Doherty RM. Diet-induced obesity and acute hyperlipidemia reduce IkappaBalpha levels in rat skeletal muscle in a fiber-type dependent manner. *Am J Physiol Regul Integr Comp Physiol* 2006;290:R233–R240
46. Bikman BT, Zheng D, Kane DA, et al. Metformin improves insulin signaling in obese rats via reduced IK Kbeta action in a fiber-type specific manner. *J Obes*. 14 January 2010 [Epub ahead of print]
47. Saito T, Jones CC, Huang S, Czech MP, Pilch PF. The interaction of Akt with APPL1 is required for insulin-stimulated Glut4 translocation. *J Biol Chem* 2007;282:32280–32287
48. Deepa SS, Dong LQ. APPL1: role in adiponectin signaling and beyond. *Am J Physiol Endocrinol Metab* 2009;296:E22–E36